ЖЭТФ, 2001, том 119, вып. 2, стр. 301–308

COULOMB EFFECTS IN SPATIALLY SEPARATED ELECTRON AND HOLE LAYERS IN COUPLED QUANTUM WELLS

L. V. Butov [ab], ***A. Imamoglu*** [ac], ***K. L. Campman*** [a], ***A. C. Gossard*** [a]

[a] *Department of Electrical and Computer Engineering and Center for Quantized Electronic Structures (QUEST), University of California, Santa Barbara, CA 93106, USA*

[b] *Institute of Solid State Physics, Russian Academy of Sciences 142432, Chernogolovka, Moscow district, Russia*

[c] *Department of Physics, University of California, Santa Barbara, CA 93106, USA*

Submitted 7 June 2000

We report on the (magneto-) optical study of many-body effects in spatially separated electron and hole layers in GaAs/$Al_xGa_{1-x}As$ coupled quantum wells (CQWs) at low temperatures ($T = 1.4$ K) for a broad range of electron–hole densities. Coulomb effects were found to result in an enhancement of the indirect (interwell) photoluminescence (PL) energy with increasing the electron–hole density both for zero magnetic field and at high fields for all Landau level transitions; this is in contrast to the electron–hole systems in single quantum wells (QWs) where the main features are explained by the band gap renormalization resulting in a reduction of the PL energy. The observed enhancement of the ground state energy of the system of the spatially separated electron and hole layers with increasing the $e-h$ density indicates that the real space condensation to droplets is energetically unfavorable. At high densities of separated electrons and holes, a new direct (intrawell) PL line has been observed: its relative intensity increased both in PL and in absorption (measured by indirect PL excitation) with increasing density; its energy separation from the direct exciton line fits well to the X^- and X^+ binding energies previously measured in single QWs. The line is therefore attributed to direct multiparticle complexes.

PACS: 71.35.-y

1. INTRODUCTION

Many-body interactions in neutral electron–hole ($e-h$) systems in semiconductor quantum wells (QWs) lead to renormalization effects [1] that were extensively studied in single quantum wells (SQWs) in the past. In particular, the main experimental features were explained by the band gap renormalization that results in a reduction of the ground state energy with increasing the $e-h$ density (see Ref. [2] and references therein).

In this paper, we study many-body effects in a system of spatially separated electron and hole layers at zero and finite magnetic fields perpendicular to the QW plane. Due to the long radiative recombination times, the $e-h$ temperatures can be much lower in this system than those achieved in single-layer $e-h$ systems. In particular, this unique property may enable the observation of a number of predicted collective phenomena [3–10]. The major difference of many-body effects in spatially separated electron and hole layers compared to single-layer $e-h$ systems is the asymmetry between the $e-e$ and $e-h$ interactions. In a set of papers, this asymmetry has been predicted to result in the instability of the uniform exciton phase at low temperatures [5, 6, 10]. In particular, condensation to an exciton liquid has been predicted for small interlayer separation: for $1.1a_2 < d < 1.9a_2$, the liquid was predicted to be metastable, while for $d < 1.1a_2$, the liquid was predicted to be in the ground state ($a_2 = \hbar^2\varepsilon/2me^2$ is the $2D$ exciton radius, ε is the dielectric constant, m is the reduced exciton mass, and $a_2 \sim 6.5$ nm for GaAs QWs) [10]. On the contrary, in another set of papers, the repulsive interaction between the indirect (interwell) excitons at low densities and the electrostatic term originating from the electric field between the separated electron and hole layers at high densities was predicted to stabilize the uniform phase in the system of separated electron and hole layers [7–9].

The spatially separated $e-h$ system with the photoexcitation-controlled $e-h$ density is realized in

electric field tunable coupled quantum wells (CQWs) (see Ref. [11] and references therein). The effects of exciton–exciton interactions at low exciton densities ($\lesssim 10^{10}$ cm^{-2}) were studied earlier [12]: an enhancement of the exciton energy with density both at zero and finite magnetic fields has been observed and interpreted in terms of the net repulsive interaction between indirect excitons (which are dipoles oriented in the z-direction).

In this paper, we report on the experimental study of the system of spatially separated electron and hole layers in GaAs/Al_xGa_{1-x}As CQW in the broad range of $e-h$ densities, up to the maximum possible $e-h$ densities corresponding to the complete screening of the external electric field in the z-direction (this maximum density depends on the applied electric field and reaches more than $2 \cdot 10^{11}$ cm^{-2} for the present experiments). The $e-h$ density was controlled by the excitation density and by the excitation energy through the absorption variation. The maximum density $e-h$ system with the minimum effective temperature was achieved at the excitation resonant to the direct (intrawell) exciton states. The experimental data suggest that the system of separated electrons and holes is uniform with the ground state energy increasing with the $e-h$ density; these data, therefore, do not support the predicted condensation to the liquid state in the entire range of $e-h$ densities that we studied.

The electric field tunable $n^+ - i - n^+$ GaAs/Al_xGa_{1-x}As CQW structures were grown by molecular beam epitaxy. A sketch of the band diagram of the structures is shown in the inset to Fig. 1. The i-region consists of two 8 nm GaAs QWs separated by a 4 nm $Al_{0.33}Ga_{0.67}As$ barrier and surrounded by two 200 nm $Al_{0.33}Ga_{0.67}As$ barrier layers. The n^+-layers are Si-doped GaAs with $N_{Si} = 5 \cdot 10^{17}$ cm^{-3}. The second sample has the same design, except for the QW widths that are equal to 15 nm. The data throughout the paper refers to the 8–4–8 nm CQW sample if not specified. The electric field in the z-direction is monitored by the external gate voltage V_g applied between n^+-layers (see Ref. [12] for details).

Because the electron Fermi level in the n^+-GaAs layers is considerably below the electron energies in the GaAs QWs, the QWs are nominally empty in the absence of photoexcitation (the concentration of the residual impurities in the QW region is unknown; however, it is certainly below the Mott density to provide free electron or hole gases in the QWs and below the density of photoexcited carriers in the CQWs studied). In most of the experiments, carriers were photoexcited by tunable cw Ti:Sapphire laser with photon energy considerably below the $Al_{0.33}Ga_{0.67}As$ barrier energy. Possible deviations from the charge neutrality occurring in the CQW electron–hole system because of different collections of electrons and holes photoexcited in the barrier layers are minimized.

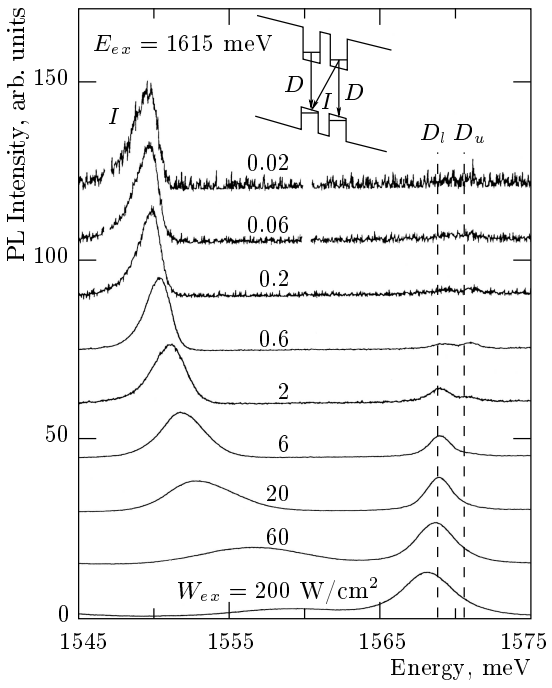

Fig. 1. Excitation density dependence of the PL spectrum at $T_{bath} = 1.4$ K, $V_g = 1$ V, and $E_{ex} = 1615$ meV. The dashed lines are a guide for the eyes. Inset: schematic band diagram of the GaAs/Al_xGa_{1-x}As CQW structure under applied gate voltage; the direct (D) and indirect (I) transitions are shown by arrows

To minimize the effect of the mesa heating, we worked with the mesa area 200×200 μm^2, which was much smaller than the sample area of about 4 mm^2. In addition, the bottom of the sample was soldered to a metal plate. The excitation was modulated with the dark-to-light ratio of about 15. The measurements were performed in a Spectromag cryostat with the bath temperature $T_{bath} = 1.4$ K. The PL spectrum was measured using a charge-coupled device camera.

2. COULOMB EFFECTS IN DIRECT AND INDIRECT PHOTOLUMINESCENCE

The separation of electrons and holes in different QWs (the indirect regime) is realized by applying a finite gate voltage that fixes external electric field in the

z-direction $F = V_g/d_0$, where d_0 is the i-layer width. The excitation density dependence of the PL spectrum in the indirect regime is shown in Fig. 1. The excitation energy $E_{ex} = 1615$ meV is sufficiently below the barrier energy to ensure the $e-h$ photoexcitation directly in QWs. The direct and indirect transitions are identified by the PL kinetics and gate voltage dependence: the direct PL line has a short PL decay time and its position is practically independent of V_g, while the indirect PL line has a long PL decay time and shifts to lower energies with increasing V_g (in the low-density excitonic regime, the shift magnitude is given by eFd, where $d \approx 11.5$ nm is close to the mean separation between the electron and hole layers) [11, 12].

Figure 1 shows that the indirect PL line monotonically shifts to higher energies with increasing the $e-h$ density; this corresponds to an increase of the ground-state energy of the spatially separated $e-h$ system. At high $e-h$ densities, the energy shift is determined 1) by the exchange and correlation energies, which results in a reduction of the energy [1], and 2) by the electric field between the separated electron and hole layers, which partially compensates for external electric field and thereby results in an increase of the energy [7, 9]. The latter contribution to the nonlinear energy shift is a unique feature of the system of spatially separated electron and hole layers and can be estimated using the plate capacitor formula $\delta E = 4\pi n_{eh} e^2 d/\varepsilon$, where n_{eh} is the $e-h$ density. The observed increase of the ground state energy of the spatially separated $e-h$ system is opposite to the case of $e-h$ plasma in SQWs, where exchange and correlation terms result in the reduction of the energy (an effect known as the band-gap renormalization [1, 2]). Therefore, in CQWs studied here, the electrostatic term dominates over the exchange and correlation terms. In particular, the observed enhancement of the ground-state energy of the system of the spatially separated electron and hole layers with increasing the $e-h$ density indicates that the real space condensation to droplets is energetically unfavorable and corresponds to the theoretical predictions of Refs. [7, 9]. On the contrary, the condensation to the exciton liquid predicted in Ref. [10] is not supported by the present experiment (we note that for the CQW studied, we have $d \approx 1.77a_2$, which must correspond to the metastable exciton liquid phase according to Ref. [10]). Indeed, if the exciton liquid were the ground state, the $e-h$ density and hence, the PL shape and energy should be fixed and independent of the excitation density; this does not correspond to the experimental data (Fig. 1).

The lowest estimate of the $e-h$ density can be obtained from the experimental shift of the indirect PL line to higher energies using the plate capacitor formula. This estimate does not include exchange and correlation terms, and the resulting value of the density is therefore lower than the actual one. In particular, the estimate for the maximum possible $e-h$ density corresponding to the complete screening of the external electric field is $\sim 2 \cdot 10^{11}$ cm^{-2} for $V_g = 1.8$ V.

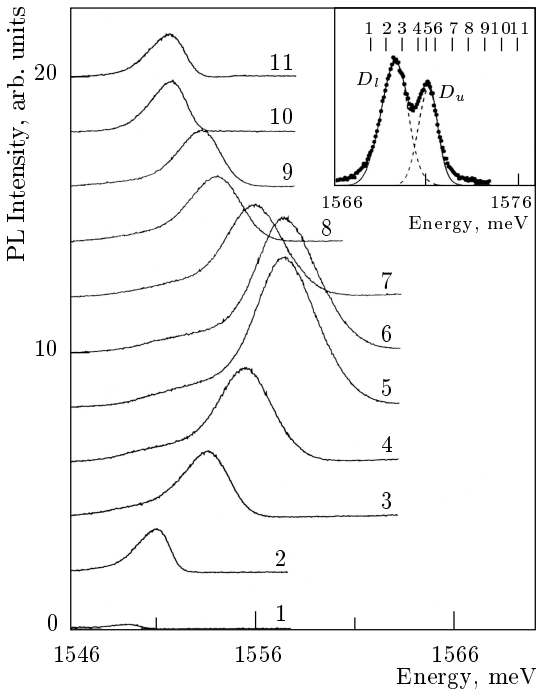

Fig. 2. Excitation energy dependence of the indirect PL at $T_{bath} = 1.4$ K, $V_g = 1$ V, and $W_{ex} = 20$ W/cm^2. The corresponding excitation energies are shown in the inset. Inset: the direct PL at $T_{bath} = 1.4$ K, $V_g = 1$ V, $W_{ex} = 0.5$ W/cm^2, and $E_{ex} = 1.96$ eV (points); for separation of the lines, the direct PL is fitted by two Gaussians (dashed lines, the sum is the solid line)

Two direct PL transitions, the upper (D_u) and the lower (D_l), are observed in the indirect regime (Fig. 1). Their excitation density dependence is opposite to that of the indirect PL line. The D_u line position is practically independent of W_{ex} and the D_l line shifts to lower energies (Fig. 1). The relative intensity of the D_l line is increased with W_{ex} (Fig. 1).

Figure 2 presents the excitation energy dependence of the indirect PL for the excitation energies in the range of direct PL (see the inset to Fig. 2). The integrated indirect PL intensity $M_0 = \int I(E)dE$ and the PL line position given by the line gravity center $M_1 = M_0^{-1} \int EI(E)dE$ are presented in Fig. 3 as a

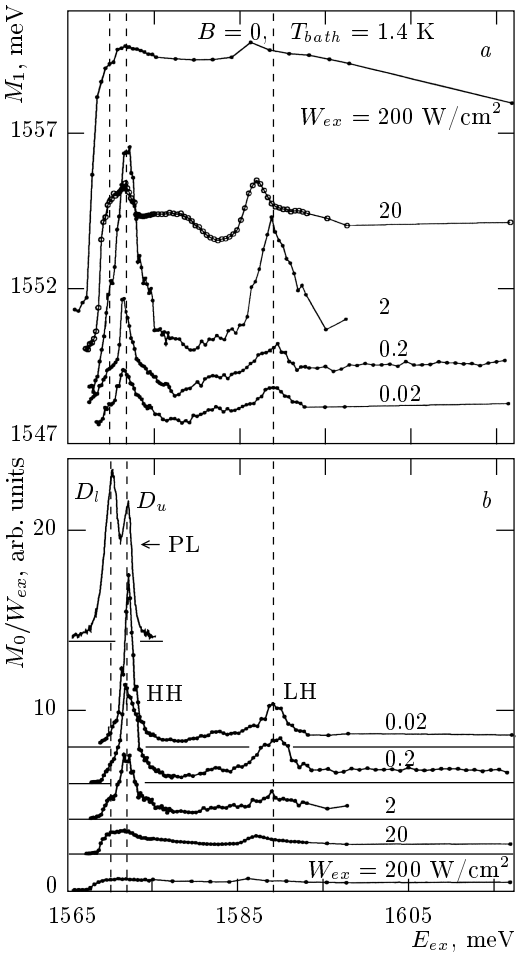

Fig. 3. Excitation energy dependence of the indirect PL line position M_1 (a) and the integrated indirect PL intensity M_0 normalized by the excitation density (b) vs excitation density at $T_{bath} = 1.4$ K and $V_g = 1$ V. The direct PL at $T_{bath} = 1.4$ K, $V_g = 1$ V, $W_{ex} = 0.5$ W/cm^2, and $E_{ex} = 1.96$ eV is shown above (b). The dashed lines are a guide for the eyes

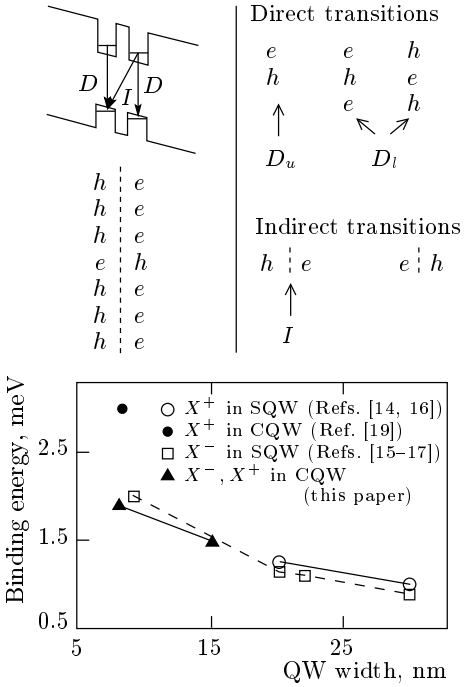

Fig. 4. Scheme of the carrier distribution in CQW in the indirect regime (left). Scheme of possible direct (intrawell) and indirect (interwell) PL transitions (right). The transition assignment (D_u, D_l, I) corresponds to that of the PL lines in Figs. 1–3; QW width dependence of X^- and X^+ binding energies in SQWs and CQWs (the lower plot)

function of excitation energies. The set of $M_0(E_{ex})$ and $M_1(E_{ex})$ dependences is a more comprehensive analog of the indirect PL excitation spectra (PLE): in addition to the latter, it contains information on a variation of the PL line position. In the case where the indirect PL dominates the $e - h$ recombination, the $M_0(E_{ex})$ dependence coincides with the absorption spectrum.

Figures 2 and 3b show that the indirect PL line intensity is maximum at the excitation energies corresponding to the D_u line. At the same time, no absorption is observed at the energy of the D_l line at low excitation densities; the absorption at the D_l line energy appears and its relative intensity increases with increasing W_{ex} (Fig. 3b).

The nature of the D_u and D_l lines is discussed in what follows. The carrier distribution scheme in CQW in the indirect regime is shown in Fig. 4 (left). The ratio of the densities of the minor carriers (electrons in the left QW and holes in the right QW) to the densities of the dominant carriers (holes in the left QW and electrons in the right QW) is proportional to the ratio between the direct and indirect PL line intensities multiplied by the ratio between the direct and indirect radiative decay times and is small[1)]. The scheme of possible direct and indirect PL transitions is evident from Fig. 4 (left) and is shown in Fig. 4 (right). We attribute the D_l line to direct multiparticle complexes because its relative intensity increases with increasing the electron–hole density in both PL and absorption (Figs. 1 and 3), which indicates that more than two particles (electrons and holes) are involved in the complex. The simplest charged complexes are X^- and X^+.

[1)] The indirect radiative decay times are in the range of tens and hundreds of ns, while the direct radiative decay time is below our system resolution, 0.2 ns [11].

The D_u line corresponds to the direct heavy hole (HH) 1s exciton, X. In CQWs, the formation of charged complexes is promoted in the indirect regime because of the interwell charge separation and the corresponding realization of the charge configuration, where the electron (hole) is surrounded by a dominant number of holes (electrons) in the left (right) QW, see the scheme of Fig. 4. Indeed, the D_l line vanishes for the symmetric charge distribution at $V_g = 0$. We note that two direct lines could be alternatively ascribed to recombination from two QWs of slightly different widths (see the inset to Fig. 1). This alternative interpretation is discarded because the lower direct line is absent in the absorption at low excitation densities (Fig. 3).

With increasing the $e-h$ density, the D_l line shifts to lower energies. This behavior of the intrawell optical transition corresponds to the band-gap renormalization in SQWs [1, 2] and is qualitatively discussed in what follows (for simplicity, we discuss the intrawell PL transitions in the right QW with excess electrons, the transitions in the left QW are characterized by a similar density dependence). At high $e-h$ densities, more than one excess electrons are in the vicinity of the photoexcited or recombining exciton. In the dense limit, the direct PL is described by the correlation effects in the $2D$ electron gas and the hole in the right QW and the $2D$ hole gas in the left QW. The PL energy of the $2D$ electron gas is reduced with increasing the electron density because of the band-gap renormalization [1]. The presence of the separated $2D$ hole gas in the left QW must further increase the PL energy reduction due to the exchange interaction with the hole in the right QW. In CQWs therefore, similarly to the SQW case, the intrawell PL energy must be reduced with increasing the density due to the band-gap renormalization. This corresponds to the experimental data (Fig. 1). We note that the X^- complex is the low-density limiting case of the correlations of $2D$ electron gas with a hole.

The correct determination of the X^- and X^+ complex binding energies must be done at the lowest $e-h$ densities to avoid the effect of extra (more than one) excess carriers occurring in the vicinity of the photoexcited or recombining exciton (see above). The binding energy of the complexes was determined from the splitting between the D_u and D_l lines at low excitation density $W_{ex} = 0.5$ W/cm^2 fitting the direct PL by two Gaussians (see the inset to Fig. 2). The evaluation of the data at the lower excitation densities results in the close values but is less accurate due to noise. The obtained binding energy of the complexes is 1.9 meV for the 8–4–8 nm CQW and 1.5 meV for the 15–4–15 nm CQW. These values are consistent with the earlier reported X^- and X^+ binding energies in the $2D$ electron (hole) gas in modulation doped GaAs SQWs: 1 meV for X^+ in 30 nm QW [13]; 1.1 and 0.9 meV for X^- in 22 and 30 nm QWs, respectively [14]; 1.15 meV for X^- and 1.25 meV for X^+ in 20 nm QW [15]; 2 meV for X^- in 9.1 nm QW [16]. The X^- and X^+ binding energies increase with reducing the QW thickness because of the enhanced Coulomb correlations, which is consistent with theoretically predicted increase of the complex stability with reduced dimensionality [17]. The binding energies of X^- and X^+ for the same QW width are close to each other [13–15, 17]. The measured complex binding energy values 1.9 and 1.5 meV for the respective 8 and 15 nm QWs fit well to the X^- and X^+ binding energy dependence on the QW width [13–17] (see the lower plot of Fig. 4). Recently, the binding energy of X^+ in the CQW structure with 8 nm QWs was reported to be 3 meV [18]; this value is also presented in Fig. 4. The difference in the binding energies observed in the CQWs with similar well and barrier widths (compare Ref. [18] and the present paper) is likely to be related to the larger amplitude of the in-plane random potential in the sample studied in Ref. [18], which is revealed in the larger PL linewidth: similarly to the case of SQWs [13–16], trions are most likely localized in CQWs by in-plane potential fluctuations; larger amplitude of potential fluctuations results in a reduction of the carrier localization area. This additional carrier confinement must enhance the Coulomb correlations and, therefore, the complex stability.

The absorption line at ≈ 17 meV above the direct $1s$ HH exciton corresponds to the direct light hole (LH) exciton (see section 3), while the shoulder at ≈ 10 meV above the direct $1s$ HH exciton corresponds to the onset of the direct excited HH exciton states $2s, 3s, \ldots$ and the HH free carrier absorption edge. This indicates a direct HH exciton binding energy about 10 meV.

Figures 2 and 3 show that the energy of the indirect PL line is locked to its intensity: $M_1(E_{ex})$ varies in phase with $M_0(E_{ex})$. This is consistent with the excitation density dependence of the indirect PL line (Fig. 1 and the excitation density dependence in Fig. 3*a*) and corresponds to the enhancement of the ground-state energy of spatially separated electrons and holes with increasing the $e-h$ density (see above). The density depends on the excitation energy due to the absorption variation.

3. SPATIALLY SEPARATED ELECTRON AND HOLE LAYERS AT HIGH MAGNETIC FIELDS

Coulomb correlation effects in the PL spectra of spatially separated electron and hole layers at perpendicular magnetic field are considered in this section. Figure 5 presents the excitation energy dependence of the indirect PL line position and the integrated indirect PL intensity vs excitation density at $B = 9$ T. These dependences are analogous to those at $B = 0$ presented in Fig. 3. At $B = 9$ T, the direct magnetoexciton lines dominate the absorption. They are identified by their magnetic field dependence presented in the inset to Fig. 5. The energy of the direct magnetoexciton is $\mathcal{E}_D(N,B) = E_g + (N+1/2)\hbar\omega_c - E_D(N,B)$, where E_g is the energy gap including the electron and hole confinement energies in the CQW, $\hbar\omega_c$ is the sum of the electron and hole cyclotron energies, N is the Landau level number, and E_D is the direct exciton binding energy; at high magnetic fields, $E_D \sim 1/l_B$ and reduces with N, where $l_B = \sqrt{\hbar c/eB}$ is the magnetic length [19]. At high magnetic fields, similarly to the zero-field case, the energy of the indirect PL increases with increasing the $e-h$ density in the entire density range (compare Figs. 3*a* and 5*a*). This is observed both with increasing excitation density and with increasing absorption (see the W_{ex} and E_{ex} dependences of Fig. 5*a*).

At high excitations, neutral dense magnetoplasma of spatially separated electrons and holes, indirect magnetoplasma, is realized: several optical transitions between occupied Landau levels of spatially separated electrons and holes (LL indirect transitions) are observed in the PL spectra and identified by their magnetic field dependences (the left inset to Fig. 6). Hot direct PL is also observed (the left inset to Fig. 6). Higher Landau level transitions appear in PL spectra with increasing excitation density because of the consequent occupation of the higher Landau levels (the right inset to Fig. 6).

The energies of all the indirect LL transitions in indirect magnetoplasma monotonically increase with increasing the $e-h$ density (Fig. 6)[2)]. This is opposite to the density dependence of direct LL transitions in SQWs where the uppermost occupied (Nth) LL transition energy is independent of the $e-h$ density in the range of filling factors $N < \nu/2 < N+1$ and is reduced with increasing the $e-h$ density everywhere outside this range because of the band gap renormalization [20]. The density dependence of direct LL transitions in SQWs is quantitatively well explained: for the uppermost occupied LLs, electrons and holes

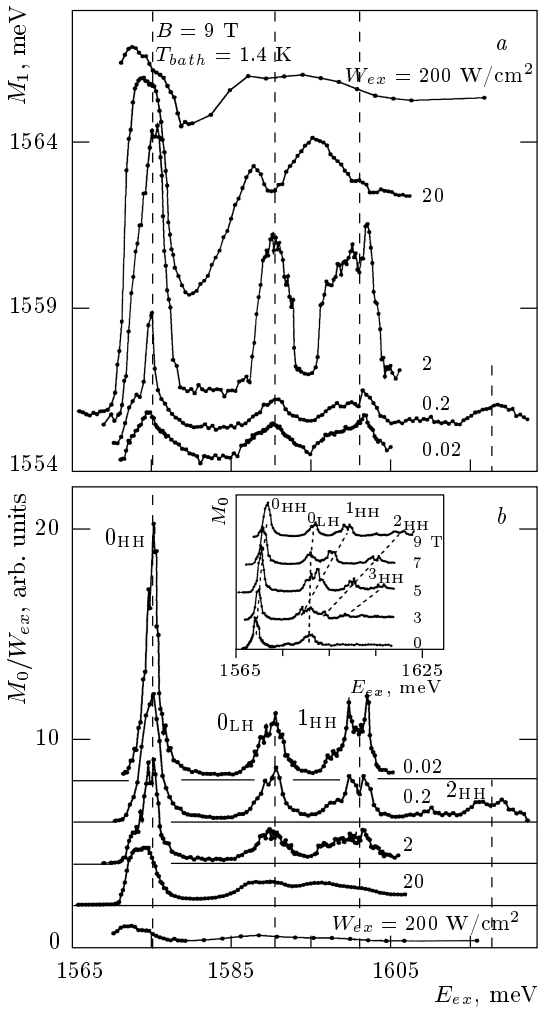

Fig. 5. Excitation energy dependence of the indirect PL line position M_1 (*a*) and the integrated indirect PL intensity M_0 normalized by the excitation density (*b*) vs excitation density at $B = 9$ T, $T_{bath} = 1.4$ K, and $V_g = 1$ V. Inset: excitation energy dependence of the integrated indirect PL intensity M_0 vs magnetic field at $T_{bath} = 1.4$ K, $V_g = 1$ V, and $W_{ex} = 0.2$ W/cm^2. The dashed lines are a guide for the eyes

[2)] The rate of the indirect PL energy enhancement reduces with increasing the excitation density (Fig. 6). The origin of this is likely to be related to a sublinear increase of n_{eh} with W_{ex}. At a higher excitation density, the internal electric field between the electron and hole layers is smaller because of the carrier screening of the external electric field (see above); at the smaller electric field, the recombination time of interwell PL becomes shorter [11], which results in a smaller density of photoexcited carriers for the fixed excitation density (in addition, at high $W_{ex} \gtrsim 20$ W/cm^2, the $e-h$ recombination time is reduced also due to the enhancement of the direct recombination).

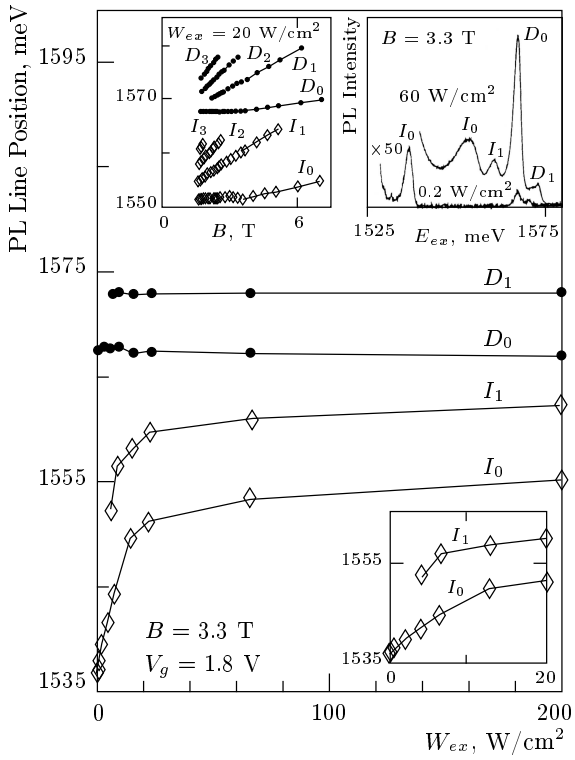

Fig. 6. Excitation density dependence of the main direct (D) and indirect (I) PL line positions at T_{bath} = 1.4 K, B = 3.3 T, V_g = 1.8 V, and E_{ex} = 1615 meV. The low W_{ex} region is expanded in the lower inset. Left inset: Magnetic field dependence of the main D and I PL line positions at T_{bath} = 1.4 K, V_g = 1.8 V, and W_{ex} = 20 W/cm^2. Upper right inset: PL spectra at W_{ex} = 0.2 and 60 W/cm^2, T_{bath} = 1.4 K, B = 3.3 T, and V_g = 1.8 V

bind into magnetoexcitons[3)] that are noninteracting in the high-magnetic-field limit because of the compensation between repulsion at small distances caused by the Pauli exclusion principle and attraction at large distances caused by the exchange interaction [21, 22]; for the filled e and h LLs ($\nu/2 > N+1$) or empty LLs ($\nu/2 < N$), the transition energy is reduced because the exchange interaction is not compensated [20, 23].

The energy independence of the direct magnetoexciton energy from density in SQWs originates from the symmetry of the $e-e$ and $e-h$ interaction [21, 22]. In CQWs, the interaction is strongly asymmetric. The asymmetry is the basis of two opposite theoretical models. According to the first model, the uniform magnetoexciton phase is unstable at low temperatures [5, 6, 10] and, in particular, the condensation to the exciton liquid is expected [10]; according to the second model, the repulsive interaction between the indirect magnetoexcitons stabilizes the uniform gas phase and the indirect magnetoexciton energy monotonically increases with density [7]. The experimentally observed enhancement of the magnetoexciton energy with density supports the second model, and, in particular, indicates the dominance of the electrostatic term over the exchange term for the spatially separated electron and hole layers (as in the zero-field case, see Sec. 2).

4. CONCLUSIONS

Many-body effects in spatially separated electron and hole layers in coupled quantum wells were found to result in an enhancement of the indirect PL energy with increasing the $e-h$ density both for zero magnetic field and at high fields for all Landau level transitions in the entire range of $e-h$ densities. This behavior is opposite to the case of electron–hole systems in single QWs, where the main features are explained by the band gap renormalization resulting in a reduction of the PL energy. The density dependence of the indirect PL energy is explained by the dominance of the electrostatic term originating from the electric field between the separated electron and hole layers; this reduces the net local electric field and results in an increase of the energy. The observed enhancement of the ground-state energy of the system of the spatially separated electron and hole layers with increasing the $e-h$ density indicates that the real space condensation to droplets is energetically unfavorable.

At high densities of separated electrons and holes, a new direct (intrawell) PL line has been observed; its relative intensity increased both in PL and in absorption (measured by indirect PL excitation) with increasing the $e-h$ density. It is therefore attributed to direct multiparticle complexes. The measured complex binding energy values 1.9 and 1.5 meV for the studied 8 and 15 nm QWs, respectively, fit well to the previously reported X^- and X^+ binding energy dependence on the QW width.

We acknowledge support from NSF Center for Quantized Electronic Structures (QUEST), INTAS, the Russian Foundation for Basic Research, and the Programme «Physics of Solid State Nanostructures» from

[3)] Note that the screening of the magnetoexciton in a dense low-temperature magnetoplasma is suppressed compared to the zero field case: in particular, in the high-magnetic-field limit, the carriers at the completely filled LLs do not participate in the screening of magnetoexcitons at the uppermost occupied LL [20–23].

the Russian Ministry of Sciences. A. I. acknowledges the support of a David and Lucile Packard Fellowship.

REFERENCES

1. S. Schmitt-Rink, D. S. Chemla, and D. A. B. Miller, Adv. Phys. **38**, 89 (1989).
2. V. D. Kulakovskii, E. Lach, A. Forchel, and D. Grützmacher, Phys. Rev. B **40**, 8087 (1989); L. V. Butov, V. D. Kulakovskii, E. Lach, A. Forchel, and D. Grützmacher, Phys. Rev. B **44**, 10680 (1991); L. V. Butov, V. D. Egorov, V. D. Kulakovskii, and T. G. Andersson, Phys. Rev. B **46**, 15156 (1992); L. V. Butov, V. D. Kulakovskii, and A. Forchel, Phys. Rev. B **48**, 17933 (1993).
3. Yu. E. Lozovik and V. I. Yudson, Zh. Eksp. Teor. Fiz. **71**, 738 (1976).
4. Y. Kuramoto and C. Horie, Sol. St. Comm. **25**, 713 (1978).
5. I. V. Lerner, Yu. E. Lozovik, and D. R. Musin, J. Phys. C **14**, L311 (1981).
6. Yu. A. Bychkov and E. I. Rashba, Sol. St. Comm. **48**, 399 (1983); Zh. Eksp. Teor. Fiz. **85**, 1826 (1983).
7. D. Yoshioka and A. H. MacDonald, J. Phys. Soc. Jap. **59**, 4211 (1990).
8. X. M. Chen and J. J. Quinn, Phys. Rev. Lett. **67**, 895 (1991).
9. X. Zhu, P. B. Littlewood, M. S. Hybersten, and T. M. Rice, Phys. Rev. Lett. **74**, 1633 (1995).
10. Yu. E. Lozovik and O. L. Berman, Pis'ma Zh. Exp. Teor. Fiz. **64**, 526 (1996); Zh. Exp. Teor. Fiz. **111**, 1879 (1997).
11. L. V. Butov, A. Imamoglu, A. V. Mintsev, K. L. Campman, and A. C. Gossard, Phys. Rev. B **59**, 1625 (1999).
12. L. V. Butov, A. A. Shashkin, V. T. Dolgopolov, K. L. Campman, and A. C. Gossard, Phys. Rev. B **60**, 8753 (1999).
13. A. J. Shields, J. L. Osborne, M. Y. Simmons, M. Pepper, and D. A. Ritchie, Phys. Rev. B **52**, R5523 (1995).
14. A. J. Shields, M. Pepper, D. A. Ritchie, M. Y. Simmons, and G. A. C. Jones, Phys. Rev. B **51**, 18049 (1995).
15. G. Finkelstein, H. Shtrikman, and I. Bar-Joseph, Phys. Rev. Lett. **74**, 976 (1995); Phys. Rev. B **53**, R1709 (1996).
16. H. Buhmann, L. Mansouri, J. Wang, P. H. Beton, N. Mori, L. Eaves, M. Henini, and M. Potemski, Phys. Rev. B **51**, 7969 (1995).
17. B. Stébé and A. Ainane, Superlatt. Microstruct. **5**, 545 (1989).
18. V. B. Timofeev, A. V. Larionov, M. Grassi Alessi, M. Capizzi, A. Frova, and J. M. Hvam, Phys. Rev. B **60**, 8897 (1999).
19. I. V. Lerner and Yu. E. Lozovik, Zh. Eksp. Teor. Fiz. **78**, 1167 (1980).
20. L. V. Butov, V. D. Kulakovskii, G. E. W. Bauer, A. Forchel, and D. Grützmacher, Phys. Rev. B **46**, 12765 (1992).
21. I. V. Lerne, and Yu. E. Lozovik, Zh. Eksp. Teor. Fiz. **80**, 1488 (1981).
22. D. Paquet, T. M. Rice, and K. Ueda, Phys. Rev. B **32**, 5208 (1985).
23. Yu. A. Bychkov and E. I. Rashba, Pis'ma Zh. Eksp. Teor. Fiz. **52**, 1209 (1990); L. V. Butov, V. D. Kulakovskii, and E. I. Rashba, Pis'ma Zh. Eksp. Teor. Fiz. **53**, 104 (1991).